From microstructural formation to early-age creep and relaxation

E.A.B. Koenders

Technische Universität Darmstadt, Germany

Institute of Construction and Building Materials

How are early age creep and relaxation linked to the microstructural formation of cementitious materials? This fundamental and extremely complex question has already being researched for many decades by considering various (combined) actions arising from chemical, physical and mechanical changes of the hardening cement-based microstructure. The current paper is prepared as part of a special session during the RILEM Week 2018, which was dedicated to the research work done by Professor Klaas van Breugel. It gives just a very brief impression of his research work done in the field of creep and relaxation, temperature development and early age cracking, and microstructure formation. The two most fundamental topics, on early age creep and relaxation, and its relation with microstructural formation, reflect his significant contributions in this field, represented by the cutting-edge results reported in two of his major deliverables, which are a TU Delft report on early age relaxation and his PhD thesis, which is on simulation of hydration in hardening cementitious materials. Based on this, a further development on the underlying mechanism is proposed for early-age stress and strain development, leading to a unified vision on relaxation, autogenous shrinkage and creep, which is confirmed by evidence achieved from experimental data on creep and relaxation from creep- and TSTM-tests.

Key words: Creep, relaxation, microstructure, autogenous shrinkage

1 Introduction

This paper provides a brief glance of the research activities of Professor Klaas van Breugel that he initiated and embraced during my stay at the Microlab, and many years beyond. During this period, he achieved major breakthroughs in the approach and application of early age creep and relaxation, and reported how to schematize and model this behaviour of concrete at various scale levels. In the beginning, his focus was on the relaxation behaviour of concrete being a fundamental phenomenon that is indispensable for an accurate assessment of the early age stress development during hardening. One of his first

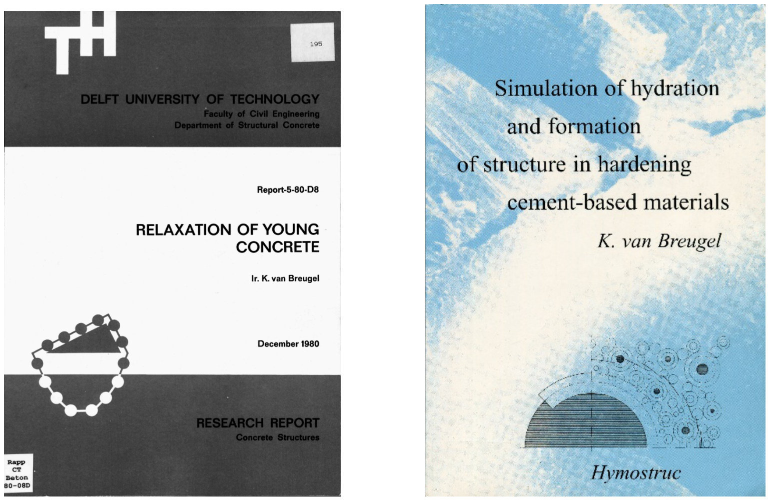

Figure 1: Left: Relaxation of young concrete, (1980), Technical report TU Delft, Author K. van Breugel [1]. Right: Simulation of hydration and formation of structure in hardening cement-based materials, (1991), PhD Thesis, K. van Breugel [2].

contributions in this field was the TU Delft research report on “Relaxation of young concrete” [1] (Figure 1, Left), where he reported a first approach to describe the relaxation behaviour of early age concrete in a fundamental way. During this period, it was very common to describe the materials behaviour in an analytical way, using mathematical formulations for the fundamental physical processes that occur, often enriched with empirical and/or phenomenological observations and descriptions. This was mainly because of the still very limited availability of computer capacity that would be necessary to model and simulate the underlying microstructural processes at a lower and more fundamental (micro-)scale level. This all changed during his PhD period (≈’85-‘91), where computer power became increasingly available and along with modern programming languages enabled it the possibility to use advanced algorithms for describing the hydrational behaviour of cementitious materials in a more precise, sequential and iterative way, making a stepwise consideration of the altering phenomena in early age cementitious materials possible. This major work became available after the defence of his PhD thesis in 1991 (Figure 1, Right), where he reported a revolutionary concept to calculate the hydration process of cementitious materials in a fundamental way operative at the microscale level. The concept combines hydration and morphology along with the formation of (micro-)structure, which he abbreviated with the acronym **HYMOSTRUC**

(**HY**dration, **MO**rphology, and **STRUC**ture development) [2]. This approach was a paradigm shift in the way a hydration process of cementitious materials could be predicted, while including various fundamental underlying processes like, particle-interactions, cement grading, cement surface area, cement chemistry, particle kinetics, temperature, water distribution and water consumption during hydration, rate dependency of available water, etc. This holistic approach was a major step forward in the way material properties of construction elements could be assessed using advanced simulation methods. The concept was a main driver for many other related developments by considering them as well from a computer-based microlevel approach. His thesis can be considered as the starting point of "computational materials" developments, which also led to an enormous enrichment of many prevailing formulations and calculations principles. The connection with his original scientific interest, being the "stress development in early age concrete" was also clear from that moment on. The evolving temperature fields in hardening concrete structures, driven by the adiabatic hydration curve of the applied concrete, could now also be calculated using computer algorithms. From there, the early age stress development in hardening concrete could be assessed by implementing his famous relaxation formula $\psi(t, \tau)$ [1] reported as:

$$\psi(t, \tau) = e^{-\left[\left(\frac{Hg(t)}{Hg(\tau)} - 1\right) + \beta . \tau^{-d} (t - \tau)^{n} \frac{Hg(t)}{Hg(\tau)}\right]} \quad (1)$$

where Hg is the degree of hydration, t time, τ the moment of loading, and β, d and n are constants depending on the type of cement and water cement ratio. This formula describes a reduction of the actual incremental stress level in a deformation imposed concrete element having a certain age at (incremental) loading. The formula applies the microstructural formation, expressed in terms of the degree of hydration, in a phenomenological way. Numerical simulations models for early age stresses could use this formula to relate changes in the progress of hydration to the evolution of the tensile strength, and to compare it with to the actual stress level in a hardening concrete element, while indicating a certain crack risk. This procedure was also followed in the Delft TEMPSPAN model for calculating the thermal stresses in early age concrete. Later this formula was challenged by Lokhorst [5], who examined the relation between deformational behaviour of sustained loaded concrete and the associated microstructural formation, which could be quantified after the launch of the HYMOSTRUC model [2]. From this, calculating the probability of cracking for a hardening concrete structure became possible using a basic level II statistical approach. Later this approach was also extended to a full level III Monte Carlo simulation model for early age cracking assessment [6].

2 Temperature development in early age concrete

The evolution of a temperature field in a hardening concrete element is driven by the reaction process between cement and water, and is correlated to the degree of hydration, which is the ratio between the actual amount of hydrated cement and the total amount of cement available in the system. The reaction process is characterised by a so-called adiabatic hydration curve, which is a unique curve for each concrete mixture. The maximum heat liberated by a concrete under adiabatic boundary conditions, is implying that no heat will disappear to the environment during hardening. This can also be measured with an adiabatic calorie meter. An example of an adiabatic hydration curve is schematically shown in Figure 2, right [1], where also two analytical formulations for this curve are presented. An adiabatic curve is a continuously ascending curve, typically indicating an adiabatic process, and representing the heat liberation with time Q(*t*). It is the source term in the differential equation of Fourier that is describing the temperature field in a structural elements` cross-section (Figure 2, left) [2]. The schematic impression (Breugel, 1980) shows a double-symmetric temperature field indicating the temperature gradients in an equally sided cross-section. Adding the heat source Q to the temperature distribution equation of Fourier, leads to the following differential equation [2]:

$$\frac{(\partial T)}{(\partial t)} = a_c * [\frac{(\partial^2 T)}{(\partial x^2)} + \frac{(\partial^2 T)}{(\partial y^2)} + \frac{(\partial^2 T)}{(\partial z^2)}] + Q(t,x,y,z) \quad (2)$$

where a_c is the temperature conduction coefficient implicitly responsible for the rate at which the temperature is distributed among the cross-section, and is depending on the degree of hydration in any location of a concrete element. The equation can be solved under consideration of the starting and boundary conditions of each individual discrete element. The output is a time dependent temperature field and the associated degree of hydration field, which both are the inputs for the stress calculation. Bedsides this, they also determine the actual state of the mechanical properties like the elastic modules and tensile strength. Along with the algorithm for calculating the early age stresses, these two modules form the kernel of the TEMPSPAN simulation code, which is the Dutch abbreviation of “Temperatures and Stresses”.

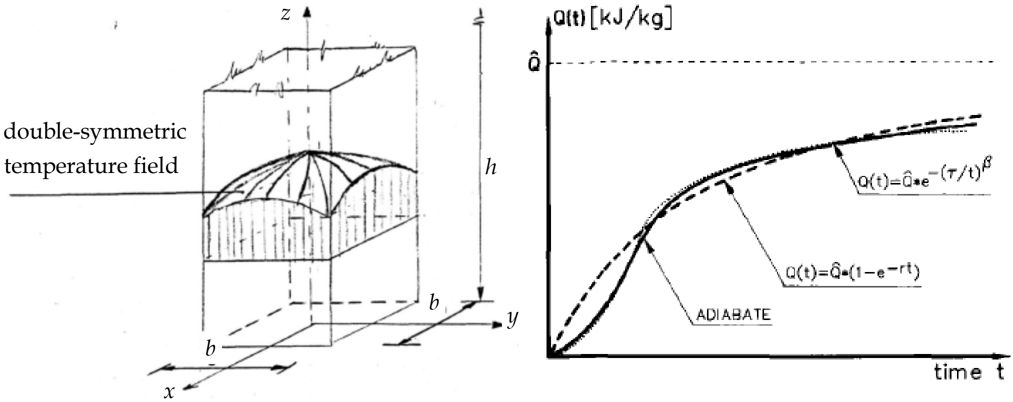

Figure 2: Left: Schematic representation of an adiabatic hydration curve with different formulas [1]. Right: Schematic handwritten plot of 2D temperature field in a column [2]

3 From temperature to stresses

Early age stresses in a hardening concrete element can be calculated by a sequential stepwise procedure. In [1], Van Breugel provided a schematic overview of the correlations between the most predominant parameter relations with time and with the degree of hydration. These are the temperature with time, the elastic modulus with time and the relaxation with time. For the relaxation behaviour of the hardening concrete, eq. 1 could be applied, along with the superposition principle that records the individual stress increments per element, consisting of a linear stress increments multiplied with the actual relaxation factor calculated according to equation 1. The involved parameters with time are schematically show in Figure 3 [1]. The resulting stress field with time can be found by summarizing all stress increments at a certain time of hardening, at a certain location in the cross-section. In this way, whenever loaded by a certain temperature field, an incremental time-dependent contribution of the total stress distribution can be calculated. In Figure 4, right, the early age stress development is schematically shown, where also the effect of relaxation is indicated. It can be observed that relaxation may be responsible for 50% of the resulting calculated tensile stresses developing inside a concrete element. The question whether the calculated early age tensile stresses also lead to early age cracking could be assessed by using various statistical approaches. In many models a level II approach is used, where the probability of cracking is calculated based on the distribution functions of the stress and the strength. Whenever the standard deviation of both parameters is known, the combined statistical probability can be calculated which indicates the result of the combined action of stress and strength in a hardening concrete system.

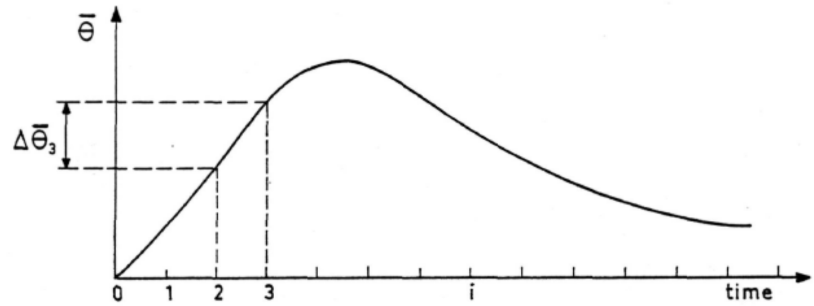

A. 10.9.1 TEMPERATURE IN A HARDENING CONCRETE BODY

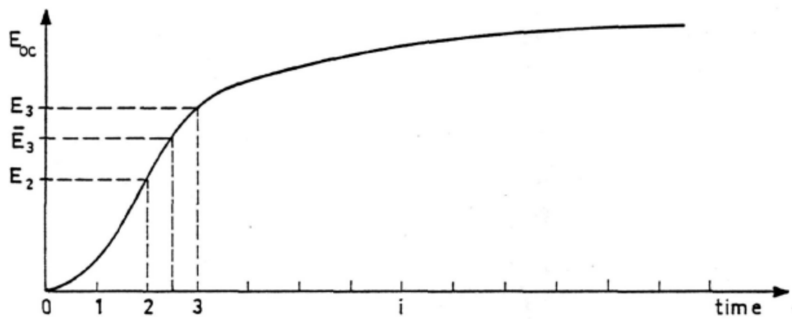

A. 10.9.2 MODULUS OF ELASTICITY

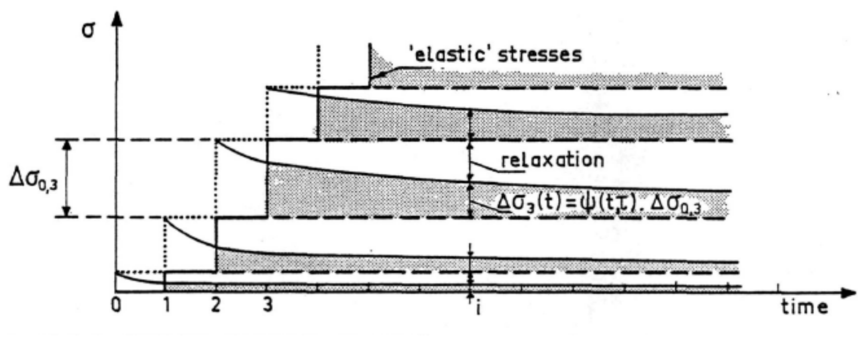

Figure 3: Schematic representation of the evolution of a temperature curve, an elastic modulus and the superposition of incremental stresses [1]

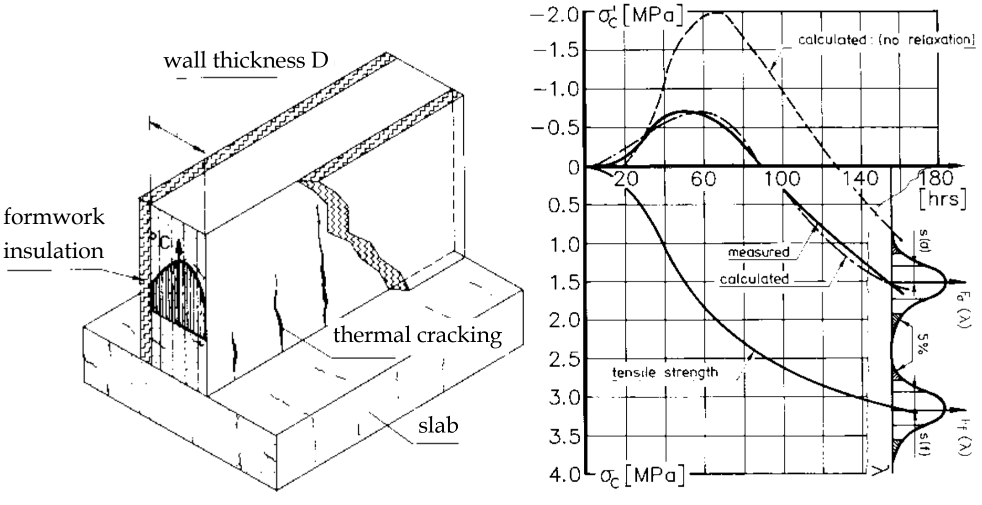

Figure 4: Left: Schematic representation of a wall with early age cracks. Right: Stress and strength development in an early age hardening concrete element [2]

4 Towards microstructure formation

A highly innovative concept on schematizing the hydration process of cement-based materials is reported by Van Breugel in his PhD thesis [2]. Although in the meantime it is already 30 years ago that he launched this breakthrough concept, it can still be considered as state of the art, and as a reference for several other hydration models that have been developed more recently [3]. Over the years, the HYMOSTRUC model has been progressively developed [4-9] and can still be considered as one of the most comprehensive micro-scale models for cement hydration capable of simulating the hydration process of Portland cement and/or blended cement systems, reaction transport, coupled nano-scale calculations and many other material related features and properties. The kernel of the HYMOSTRUC model is very divers and consists of either a statistical-based stacking model for the particle structure as well as of a fully random stacking for the various particle gradings involved in the cementitious system. This can be cement in combination with any type of pozzolan, air bubbles and/or any other kind of particle. Initially, the model considers the particles to be spherically shaped and each having their own reaction chemistry and kinetics, driven by the local moisture and packing conditions. Latest developments also consider irregular shaped particles and with complex thermodynamics [9]. Hydration products growing in outward direction and are able to embed other smaller particles in their expending outer shell [2] (Figure 5). During this

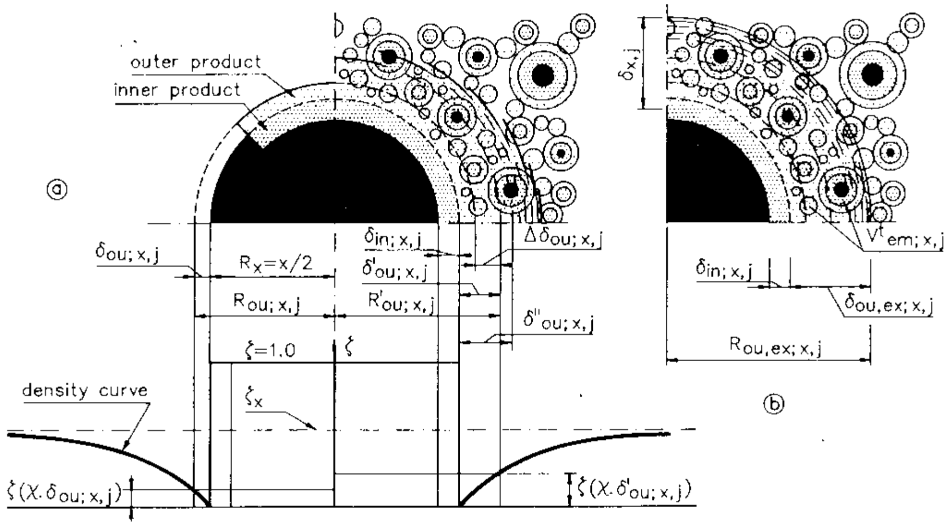

Figure 5: Particle expansion mechanism of the HYMOSTRUC model proposed by Van Breugel [2]

continuous series approach, a successive progression of the expanding outer shell develops leading to a final stage, with a shell of fully or partly hydrated particles embedded, that mimics a virtual cementitious microstructure. Figure 5 shows the original representation of this approach [2], where Figure 6 shows the results of one of recent versions of the HYMOSTRUC model. Left is plotted the initial stage of a blended particle structure [11]. Middle shows the hydrated blended particle structure containing various phases [10], and Right, shows the transport of moisture through the capillary pore space [11]. The results show the so-called virtual microstructures that can be analysed by the model's 3D viewer using a voxelisation mode being a digitalisation of the particle-based virtual

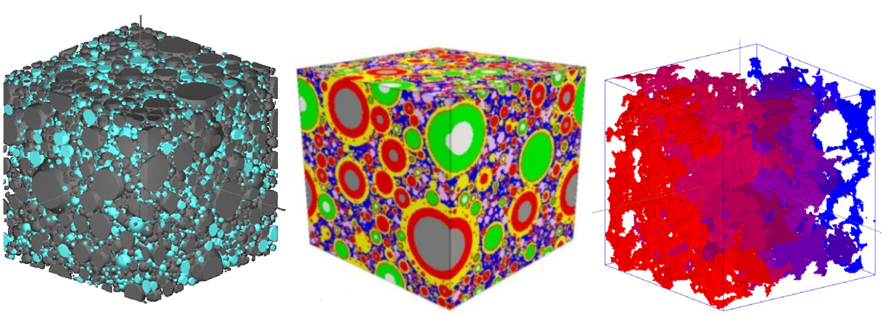

Figure 6: Results of HYMOSTRUC model. Left: Blended particle structure at initial stage [10]. Middle: Blended particle structure after hydration has ceased [9]. Right: Transport of capillary water through the developing pore structure of the hydrating microstructure [11]

microstructure. This enables a detailed analysis of the achieved morphology and state of the hydrated phases as well as an analysis of the pore structure. This latter also includes a floodfill algorithm with which the pore connectivity inside a hydrating microstructure can be evaluated continuously, while it can also be used to determine whenever the capillary pores become disconnected and lose their ability to transport capillary water throughout the pore system. This issue is of particular importance for durability assessments of concrete members exposed to harsh environments. The simulation of the hydration evolution enables also the opportunity to analyse the stiffness of the microstructure in combination with the internal capillary stresses. This process introduces the ability of the model to simulate viscoelastic properties like creep and shrinkage. This was initially done by Lokhorst [5], and will be further discussed in the next sections.

5 From microstructure formation to early-age relaxation

During the hydration process, the pore water, which is accumulated in the evolving pore space, will be consumed by the cement reaction causing a so-called internal drying or self-desiccation. This internal drying process drives the development of capillary stresses that are evolving at the menisci between the capillary pore water and the pore walls of the

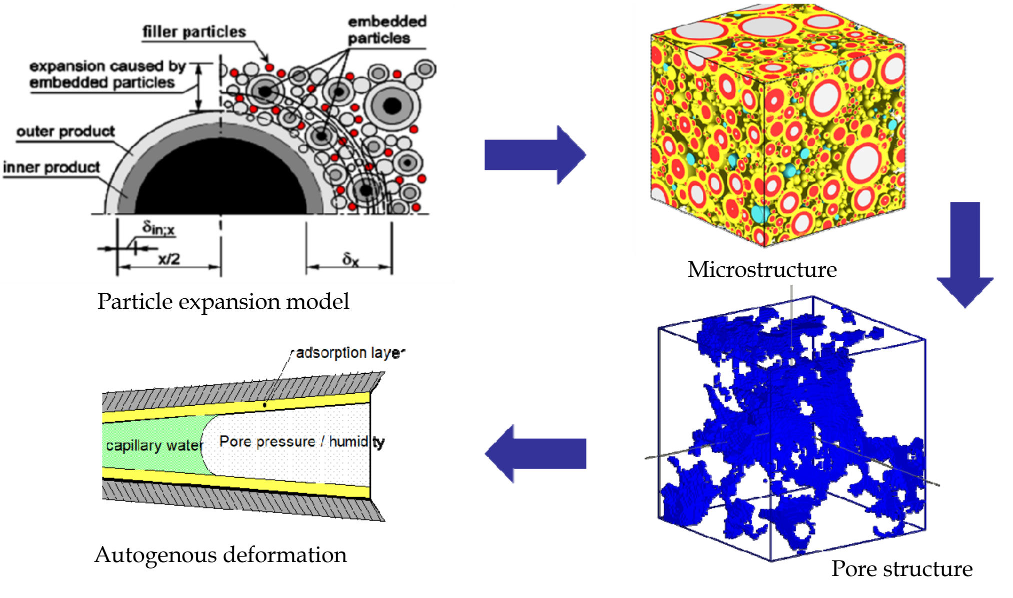

Figure 7: Schematic representation of the built up from particle structure, to microstructure, to pore structure, to internal capillary stresses and autogenous deformation

emptied pore space. These stresses develop with progress of the hydration process and are, therefore, strongly correlated to the formation of microstructure, the associated consumption of pore water, and to the emptying pore space. The stresses are acting on the evolving microstructure as an internal contraction force, where it induces a volumetric shrinkage of the hardening cementitious paste. In particular for a regular concrete, these internal contraction deformations will be restraint by the aggregates, which due to a significantly higher stiffness, will lead to a reduction of the external strains. This reduction of internal deformations due to self-desiccation can be measured under laboratory conditions from specimens, or can be simulated by a computer model (Figure 8).

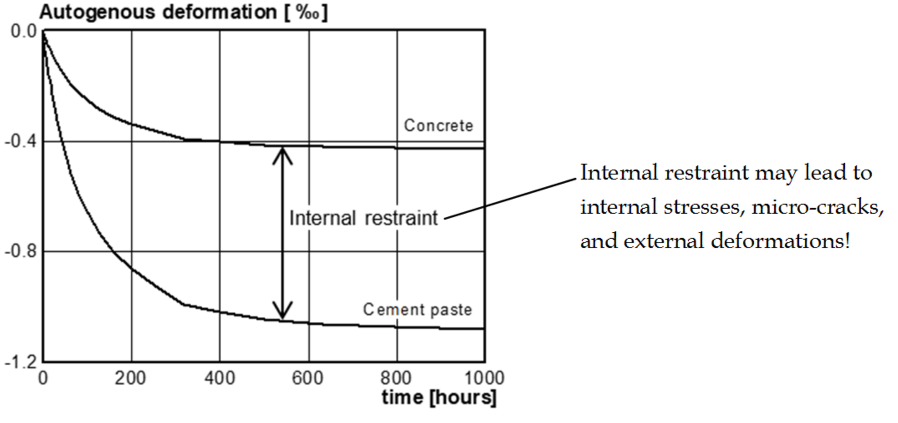

Figure 8: Schematic representation of autogenous deformation of cement paste without aggregates and of concrete with aggregates added. The difference in deformation shows internal restraint [4].

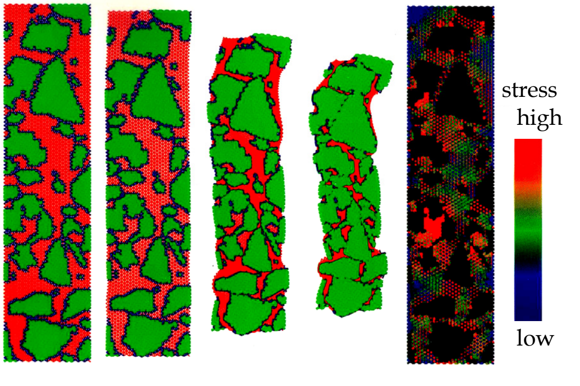

Figure 9: Schematic representation of autogenous deformation of a prismatic concrete specimen. Left: Four sequential steps showing the progressive development of autogenous deformation, and Right: The corresponding tensile stresses that developed in the cement paste [4]

As the contraction coincides with the actual state of moisture in the pore structure of the evolving microstructure, a correlation with the pore size distribution and the water cement ratio seems to be appropriate. Meaning that the relative humidity of the emptied pore space could be a clear indicator for the state of internal deformation of hardening cementitious systems. This trend has also been confirmed by many researchers among which [3],[5],[12]. Along with this, it would be interesting to see to what extend stresses are being build up whenever restraining a concrete specimen loaded by contraction due to self-desiccation. These experiments can be conducted with a so-called Thermal Stress Testing Machine (TSTM), which is a advanced way to measure the actual deformations of a hardening concrete starting directly after casting (Figure 10). For a regular C65 concrete with a water cement ratio of 0.4 two tests were conducted. In the first test (Figure 11, left),

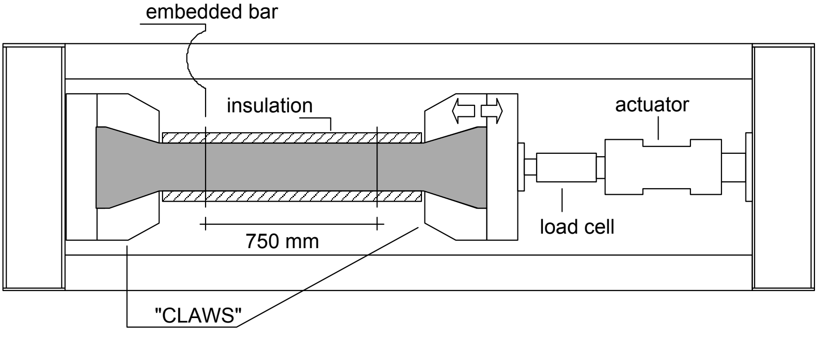

Figure 10: Schematic representation of a Thermal Stress Testing Machine (TSTM) for measuring self-desiccating stresses or deformations on sealed and thermally controlled hardening specimens

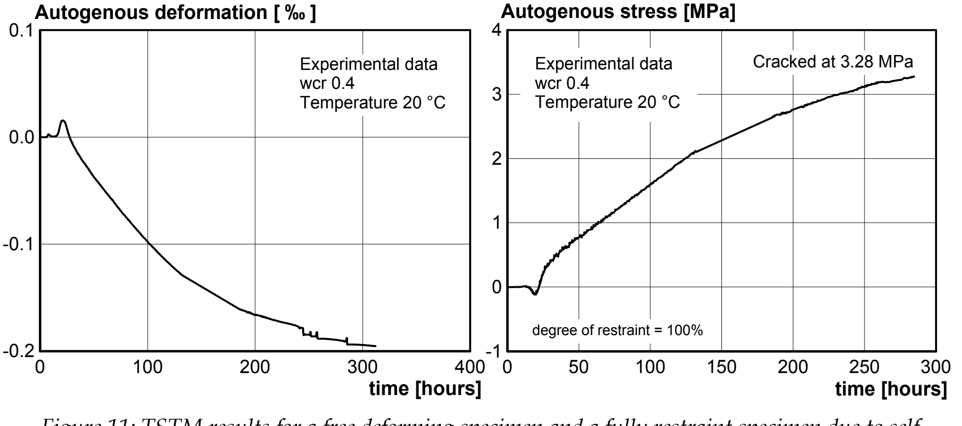

Figure 11: TSTM results for a free deforming specimen and a fully restraint specimen due to self-desiccating stresses, also indicated as autogenous stresses, under sealed conditions [4]

the specimen could freely deform while the contraction deformations evolved during hardening were recorded continuously with time. In a second test (Figure 11, right), applying the same concrete and same thermal conditions, all autogenous contracting deformations were restraint, by recording the force needed to comply with this full restraint condition. The result of these two measurements is provided in Figure 12, showing a stress-strain curve representing the constitutive behaviour of an autogenously

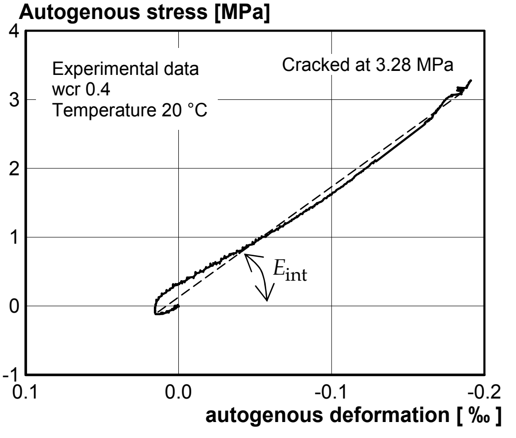

Figure 12: Autogenous stress versus autogenous strain measured on a full restraint TSTM specimen, under sealed conditions and constant temperature of 20 °C [4]

deforming TSTM specimen under full restraint. From this figure, the following (roughly linear) relationship between the autogenous stress and autogenous strain can be assumed as follows:

$$\sigma_{au} = E_{\text{int}} \cdot \varepsilon_{au}$$

$$E_{\text{int}} \approx \frac{3.2}{0.2 \cdot 10^{-3}} = 16 \text{ GPa}$$

where σ_{au} is the autogenous stress, ε_{au} the autogenous strain, and E_{int}, the so-called internal viscoelastic modules which, depending on the fit, ranges between 15 and 18 GPa [13]. The interpretation of the autogenous stress-strain curve feeds the impression that the constitutive behaviour of autogenous shrinkage in concrete shows an almost intrinsic linear elastic behaviour, and that a reduction of these stresses due to relaxation cannot be observed. This would imply that stress relaxation in early age concrete under an autogenous (and/or thermal) contraction would not evolve and that the actual stress level in the hardening concrete can simply be calculated using a linear constitutive relationship.

Further pathfinding work in this field has been done by Hansen et.al. [13], and Rossi [14], where strong evidence for a linear relation between the viscoelastic response (creep and relaxation) of sealed concrete was also recorded using different measuring techniques (Figure 13). A further interpretation of the driving force behind this linear elastic behaviour can be attributed to the internal capillary forces that develop inside the desiccating pore structure. Progressive hydration enhances the capillary stresses inside the narrowing pore-structure causing a contracting strain to the cementitious microstructure, and, ones restraint, will lead to imposed stresses. This process shows an intrinsic linear behaviour between stress and strain. For finer pore structures, meaning lower water-cement ratio systems, the evolving capillary stresses due to hydration will be higher, but ones restraint, the stresses will also be higher. Meaning that this internal restraint of an evolving concrete shows an inherent linear constitutive behaviour, which is only depending on the fineness of the evolving pore structure configuration that determine magnitude of the associated capillary stresses. It also implies that the relative humidity inside the emptied pore space is the most appropriate parameter that would determine the order of magnitude of the stresses that develops whenever restraining an early age concrete. This interpretation means that, when we observe early age relaxation, this is in fact autogenous shrinkage.

When going back to the TSTM as an appropriate experimental device that enables measuring the hardening stresses along with the complementary strains (with a so-called

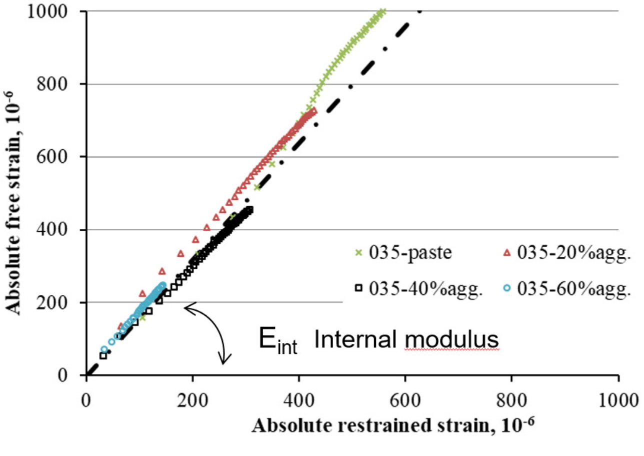

Figure 13: Autogenous stress versus autogenous strain for various concrete mixtures showing a constant linear elastic constitutive behaviour [13]

dummy specimen [5]), the validity of the proposed approach can be evaluated. For this a second test with the same mixture has been analysed. The test is conducted under semi-adiabatic conditions, meaning that in the TSTM specimen stresses have developed due to both temperature and autogenous shrinkage (see Figure 14). On the left hand side the measured temperature evolution of a hardening concrete TSTM specimen is presented. On the right hand side, the measured associated hardening strains are shown, where both strain contributions are also separated into a thermal strain and an autogenous shrinkage strain. For this, the thermal strains is calculated from the temperature evolution using a thermal expansion coefficient of 1.2E-5 m/m. The results show an increase in temperature up to 43 °C after about 20 – 25 hrs, followed by a decline to the environmental temperature of the testing condition, which is 22 °C. From this, a hardening strain ε_h up to the moment of cracking of ca.0.19 ‰ can be observed, followed by an autogenous contraction of the specimen up to a level of ca. -0.2 ‰ that was measured until 120 hrs. From this data the associated early-age stresses can be calculated according to the proposed internal modulus concept. For this specimen a stress of 2.97 MPa was measured at cracking (see Figure 15). In order to calculate this early age stress at cracking two different routes can be followed. When assuming that the internal modules is also applicable for thermal deformations in tension, the actual tensile stress in the specimen can be calculated directly from 1) the measured hardening strains ε_h , which represents the summation of the thermal and autogenous strain. Alternatively, 2) the thermal strain ε_T and autogenous strain ε_{au} can be

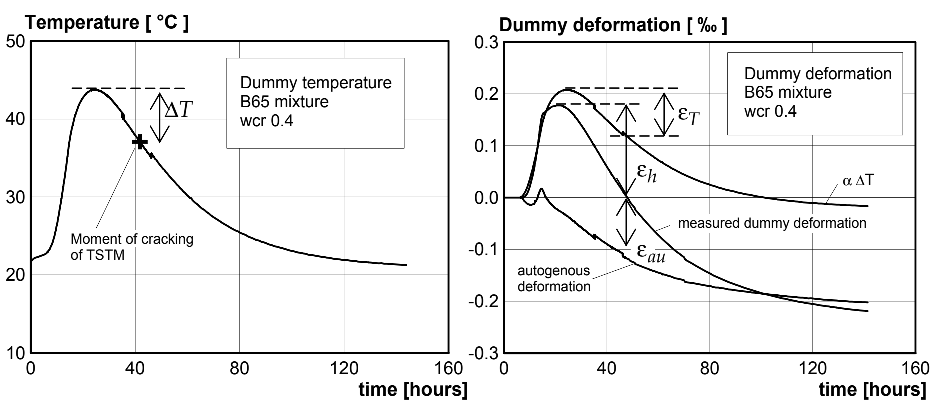

Figure 14: Left: Semi-adiabatic temperature development measured in the TSTM specimen during hardening. Right: Autogenous shrinkage strains and total load independent deformation that developed during hardening in the complementary dummy (control) specimen [15]

considered separately, as presented in Figure 14. From this, a first order calculation can be made to assess the early age stresses in the hardening specimen:

1): $\sigma = \varepsilon_h \cdot E_{\text{int}} = 0.19E-3 \cdot 16 \text{ GPa} \cong 3.2 \text{ MPa}$

2): $\sigma = (\varepsilon_{au} + \alpha \cdot \Delta T) \cdot E_{\text{int}} = (0.12E-3 + 1.2E-5 \cdot (44-37)) \cdot 16 \text{ GPa} \cong 3.26 \text{ MPa}$

The results show very good agreement with the results of the measured stress development in the specimen during hardening as presented in Figure 15. As cracking occurred at nearly 3 MPa, the calculated results also compensate for the stresses in compression. A more accurate calculation can be achieved when implementing this concept in a computer code. The results confirm the impression that this internal linear elastic modulus can indeed be applied to estimate the hardening stresses that develop in early age concrete. More research is needed to determine the validity range of this concept for various types of concretes and mortars. However, due to the intrinsic nature of the development of an internal modulus in a hardening concrete due to autogenous shrinkage, it is expected that the concept would be widely applicable in early-age concrete mixtures.

6 What about creep?

You could ask yourself the question “is this all really true?”, since we are used to the fact that relaxation of concrete is a viscoelastic driven stress reduction in early age concrete that takes place during an imposed deformation under confined conditions. In fact, it would

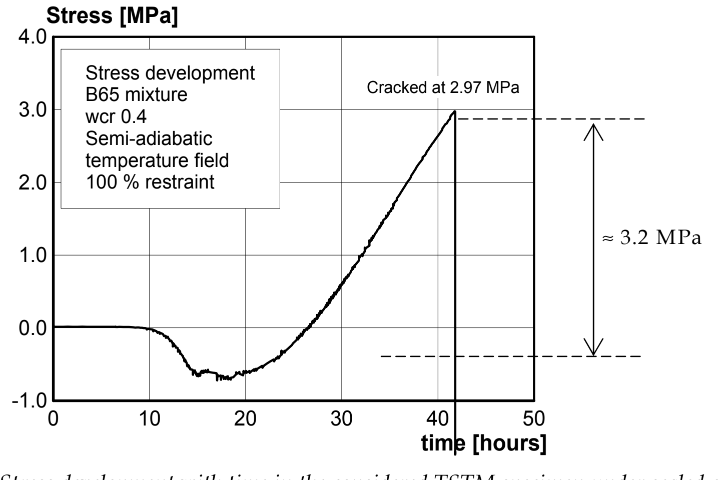

Figure 15: Stress development with time in the considered TSTM specimen under sealed conditions

also be possible to go a step further, by evaluating creep under sustained loading conditions. This could be an interesting exercise since relaxation and creep are reciprocally connected to each other. In a way, the question is whether creep under sustained loading is also related to autogenous shrinkage in a similar way relaxation is. Or in other words, is it autogenous shrinkage we measure if we think we measure creep? In order to evaluate this, creep tests were re-evaluated to see their deformation under sealed conditions, and under 20% and 40% load level (rate 3 kN/s or 0.3 MPa/s) with respect to the actual strength of the loaded specimen (Figure 16). The mix design, used for the evaluated creep tests, is presented in Table 1, showing a regular blended concrete with a water to cement ratio of 0.4. The specimens consisted of prisms with dimensions 10x10x40 cm, which were moisture sealed directly after demoulding with two layers of aluminium foil, which was also kept in that way during elapse of the creep test. This was done for the actual creep specimen as well as for the control specimen, which was not loaded and was only there to record the load independent deformations. These load independent deformations were measured from this sealed control specimen, and was located in the close vicinity of the sustained loaded creep specimen. Figure 17 shows the results of several specimens, which started after 24, 48 and 96 hours of age. The measured total strain represents the autogenous strain and the thermal strain of the sealed specimen. The accompanying creep results measured after loading at 24 and 48 hrs are presented in Figure 18. In these results show the "elastic + creep strain" along with the load independent "shrinkage strain" caused by autogenous deformation and thermal effects measured during the creep measurement (here 228 and 216 hours for 24 and 48 hrs of loading age, respectively). From

Table 1: Mix design of the evaluated creep specimens [15]

Mixture	Unit	B65	Note
Cement	kg/m^3	300	CEM III /B42.5 (CEMY)
	kg/m^3	100	CEM I 52.5 R (ENCI)
W/C		0.40	Water/Cement ratio
Aggregates			
0 – 4 mm	%	46	Fine aggregate (sand)
0 – 16 mm	%	54	Coarse aggregates
Liquid 1	%	0.4 – 0.6	Lignosulfonaat
Liquid 2	%	0.7 – 1.5	Naphtaleensulfonaat
Air content	%	2.5	maximum

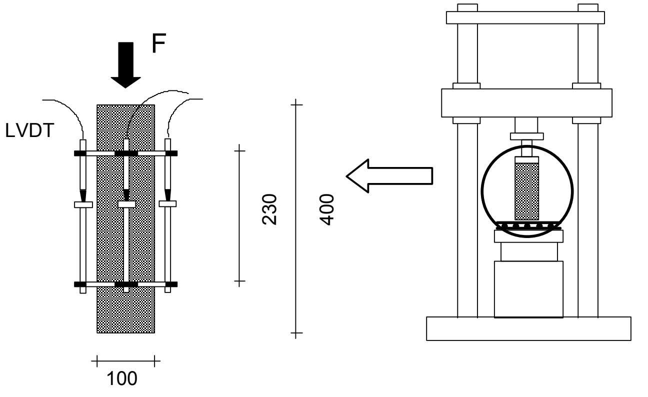

Figure 16: Creep setup with a detailed view of the LVDT configuration. For both the control and the creep specimen, the deformations were measured with a similar LVDT configuration [15]

Table 2: Compressive prism strength at loading for the 20% and 40% series [15]

Age [hours]	Compressive strength of prisms [MPa] 20% series	Compressive strength of prisms [MPa] 40% series
24	11.6	10.5
48	22.6	22.3

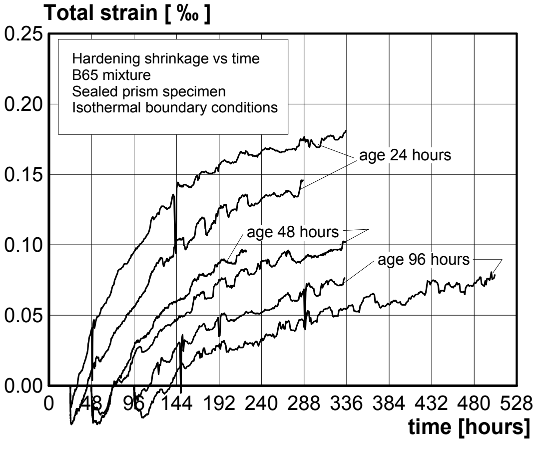

Figure 17: Load independent deformations of prism specimens. Measurements started after 24, 48 and 96 hours of age, sealed conditions [15]

the results in Figure 18 it can be observed that shortly after the deformations in the specimen have stabilized, the increase of the creep strains with time is zero. This can be observed for both loading ages, i.e. 24 and 48 hrs. In a way, this means that after subtracting the load independent shrinkage deformations from the originally measured total creep strain, a horizontal line exists for the creep strain curve, representing the fact that the measured creep strain is exactly similar to the measured load independent deformation, which is represented by the autogenous shrinkage. The thermal strains of the creep and control specimen complement each other and will not affect this result.

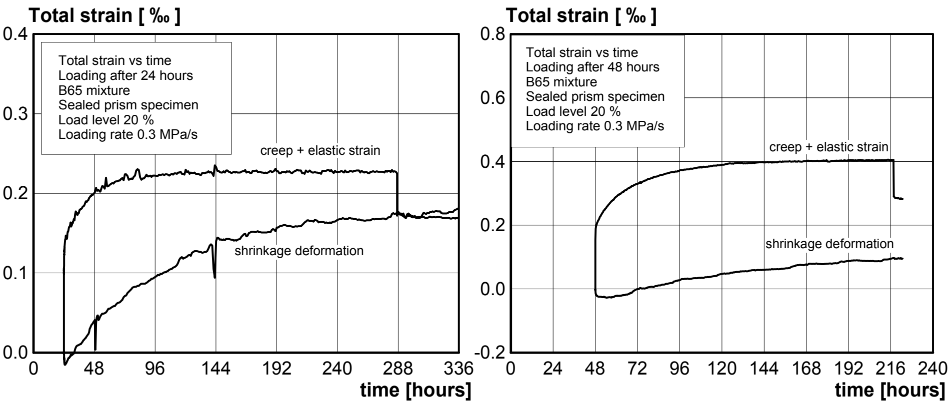

Figure 18: Total strain results (elastic + creep) measured on a sealed prism specimen loaded (20%) after 24 and 48 hrs of age, and load independent shrinkage strain measured from control specimen

This remarkable observation supports the impression that it is in fact autogenous shrinkage what we measure when we think we measure creep. Higher loading levels up to 40% of the actual strength at loading also shows similar results. In Figure 19, the total elastic + creep strain, along with the load independent shrinkage strain is presented for a load level of 40%. After a stabilization period, the results show also a complete horizontal line for the creep curve indicating a complementarity between the creep strains and the load independent autogenous shrinkage strains. This observation supports the mechanism discussed in the previous section, implying that what we observe as creep and/or relaxation is in fact autogenous shrinkage driven by microstructural self-desiccation.

Another point of interest is the so-called stabilisation period that occurs directly after (elastic) loading of the specimen, in this case, after 24 and 48 hours, and ends where the strains reach the horizontal platform. Due to the evolving autogenous shrinkage strains

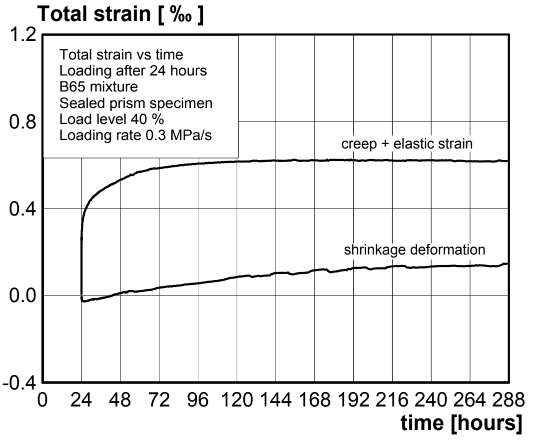

Figure 19: Total strain results (elastic + creep) measured on a sealed prism specimen loaded (40%) after 24 hrs of age, and the load independent shrinkage deformation from the control specimen

until loading, tension stresses will build up in the cement paste due to the restraining effect the aggregates have on the contracting cement paste. After applying the creep load, this stress state will change, and the paste will turn into compression again, causing a redistribution of the internal stresses, that takes place over a certain period of time. Because of this, for those specimens loaded after 24 hours (less autogenous strain built up), this redistribution period will be shorter than those loaded after 48 hours of even at later age, since the actual level of autogenous shrinkage built up till that time has to be redistributed will be larger for older specimens. This difference in redistribution time can also be observed from Figure 18 and Figure 19.

7 Discussion and conclusions

The first sections of this paper provide just a brief glance of the work conducted by Professor Klaas van Breugel on early age relaxation and micro-level hydration modelling during his early life in research, followed by a further development of his work, leading to a unified vision on relaxation, autogenous shrinkage and creep. In the early years, thermal cracking in concrete at early ages was among the main research topic that gained full attention of the scientific research community. Today, various topics related to this research area are still opportune and still under development by many researchers all over the world. One of the major topics in this field that is still largely undisclosed, and still open for new path-finding developments, is on the mechanism that drives relaxation and creep of concrete at early-ages. A link of these phenomena to the hydration driven changes of the microstructure was already launched in the mid-nineties, as a conceptual approach, which turned out to be very promising. The main research lines initiated by Van Breugel, all followed the degree of hydration as the main parameter that describes the actual state of the microstructure, in terms of morphology, hydration, solidification and porosity, and he called it the "backbone" of a hardening cementitious system. The degree of hydration can be measured experimentally in various ways, but with the launch of the HYMOSTRUC model, the progress of hydration and associated microstructure could also be simulated numerically in a very convenient and efficient numerical way. The direct link between the microstructural formation and the state of moisture in the evolving pore structure opened the way to consider microstructural deformations as a phenomenon that is driven by the internal capillary stresses. This enabled the possibility to describe autogenous shrinkage as a function of the relative humidity in the pore space, which is generally known as s self-desiccation process that introduces capillary stresses that act internally on the evolving microstructure. With this, an inherent contraction of the microstructure will emerge, which is strongly depending on the state of moisture in the capillary pore space initiated by the water to cement ratio and the fineness of the cement. In fact, it is a geometrical driven phenomenon that is, therefore, largely independent of other cement-related parameters. When considering this mechanism in a wider context, other early-age phenomenon might be related, or even be driven by these inherent self-desiccation deformations. In a way, it turned out that the relationship between autogenous strains and autogenous stresses measured from a hardening concrete TSTM specimen showed a nearly linear elastic behaviour, which is inherently related to the pore structure geometry and its state of moisture (resembled by the capillary stresses). Meaning that this mechanism does not show any stress reducing phenomenon that would support the existence of a viscoelastic stress release such as stress relaxation. Further development of this observation enabled it to assess the evolving early age stresses emerging from a hardening concrete element directly from the hardening or thermal plus autogenous strains multiplied with a so-called internal modulus, which can be measured from the relationship between the autogenous stresses and autogenous strains. In a way, the results of a simple hand calculation turned out to be very promising and support the concept of the existing linear internal modulus. Moreover, when applying an analogical approach of the proposed internal self-desiccation driven deformation concept to creep, a comparable relation with the autogenous shrinkage strains emerge. For a sustained loaded sealed specimen, and corrected for load independent deformations caused by thermal and autogenous strains, no viscoelastic creep strains develop, showing a horizontal plateau in the creep curve, indicating no increase in creep deformation. This actually implies that the creep strains are identical to the autogenous strains, since the thermal deformations of both the control and creep specimen complement each other. This remarkable observation would mean that what we observe as creep is in fact autogenous deformation. The presented vision and observations are based on a much larger number of tests than reported in this paper. However, more experimental results would still be recommended to fully understand the range of applicability of the proposed unified vision on relaxation, autogenous shrinkage and creep.

References

[1] Breugel, K. van, (1980), Relaxation of young concrete, Report-5-80-D8, TU Delft.

[2] Breugel, K. van, (1991), *Simulation of hydration and formation of structure in hardening cement-based materials*, (1991), PhD Thesis, TU Delft.

[3] Dolado, J.S. & van Breugel, K. (2011). Recent Advances in Modeling for Cementitious Materials. *Cem and Con Res*. 41. 711-726. 10.1016/j.cemconres.2011.03.014.

[4] Koenders, E.A.B., (1997), *Simulation of volume changes in hardening cement-based materials*, PhD Thesis, TU Delft, The Netherlands.

[5] Lokhorst, S.J., (1999), Deformational behaviour of concrete influenced by hydration related changes of the microstructure, TU Delft report 5-99-05.

[6] Ham, H.W.M., (2011), *Microstructure and transport phenomena in viscoelastic modelling of hardening cementitious materials*, PhD Thesis, TU Delft, Netherlands.

[7] Zule, M.S., (2003), *Effect of reinforcement on early age cracking in high strength concrete*, PhD Thesis, TU Delft, The Netherlands.

[8] Ye, G., (2003), *Experimental Study and Numerical Simulation of the Development of the Microstructure and Permeability of Cementitious Materials*, PhD Thesis, TU Delft.

[9] Peng Gao, (2018), *Simulation of hydration and microstructure development of blended cements*, PhD Thesis, TU Delft, The Netherlands.

[10] Koenders, E.A.B., Hansen, W., Ukrainczyk, N., Toledo-Filho, R., (2014). 'Modeling Pore Continuity and Durability of Cementitious Sealing Material', *Journal of energy resources technology*. 136(4) (2014) 042906:1-11.

[11] Ukrainczyk, N., Koenders, E.A.B., (2014) 'Representative elementary volumes for 3D modeling of mass transport in cementitious materials', *Modelling and simulation in materials science and engineering*. 22(3) (2016) 035001:1-24.

[12] Lura, P., *Autogenous Deformation and Internal Curing of Concrete*, PhD Thesis, TU Delft, The Netherlands.

[13] Hansen, W., Liu, Z., and Koenders, E.A.B., Internal Viscoelastic Modulus Associated with Autogenous Shrinkage in *Cementitious Materials, Journal of Advanced Concrete Technology*, Vol 12, 496-502, Nov. 2014.

[14] P. Rossi, J.-L. Tailhan, F. Le Maou, L. Gaillet and E. Martin, Basic creep behavior of concretes investigation of the physical mechanisms by using acoustic emission, *Cement and Concrete Research*, Volume 42, Issue 1, January 2012, Pages 61-73.

[15] Koenders E.A.B., (1997), Experimenteel onderzoek naar het krimp- en kruipgedrag en naar de spanningsontwikkeling tijdens de vroege fase van het verhardingsproces, TU Delft Internal report nr. 25.5-97-1.